Proc. Natl. Acad. Sci. USA
Vol. 80, pp. 4012–4016, July 1983
Cell Biology

110

Photoelectron microscopy and immunofluorescence microscopy of cytoskeletal elements in the same cells

(microfilament/intermediate filament/Pt K2 epithelial cell/Rat-1 fibroblast)

KAREN K. NADAKAVUKAREN*, LAN BO CHEN*, DOUGLAS L. HABLISTON†, AND O. HAYES GRIFFITH†

*Dana-Farber Cancer Institute, Harvard Medical School, 44 Binney Street, Boston, Massachusetts 02115; and †Institute of Molecular Biology, University of Oregon, Eugene, Oregon 97403

Communicated by Harden M. McConnell, March 28, 1983

ABSTRACT **Pt K2 rat kangaroo epithelial cells and Rat-1 fibroblasts were grown on conductive glass discs, fixed, and permeabilized, and the cytoskeletal elements actin, keratin, and vimentin were visualized by indirect immunofluorescence. After the fluorescence microscopy, the cells were postfixed and dehydrated for photoelectron microscopy. The contrast in these photoelectron micrographs is primarily topographical in origin, and the presence of fluorescent dyes at low density does not contribute significantly to the material contrast. By comparison with fluorescence micrographs obtained on the same individual cells, actin-containing stress fibers, keratin filaments, and vimentin filaments were identified in the photoelectron micrographs. The apparent volume occupied by the cytoskeletal network in the cells as judged from the photoelectron micrographs is much less than it appears to be from the fluorescence micrographs because the higher resolution of photoelectron microscopy shows the fibers closer to their true dimensions. Photoelectron microscopy is a surface technique, and the images highlight the exposed cytoskeletal structures and suppress those extending along the substrate below the nuclei. The results reported here show marked improvement in image quality of photoelectron micrographs and that this technique has the potential of contributing to higher resolution studies of cytoskeletal structures.**

Photoelectron microscopy (photoemission electron microscopy or PEM) has recently been introduced into the study of whole cells (1, 2) although the origins of this technique are old, predating both transmission electron microscopy and scanning electron microscopy (for review, see ref. 3 for physics and refs. 4 and 5 for biological applications). Photoelectron microscopy differs significantly from the established techniques of transmission and scanning electron microscopy even though the image is formed by electrons. The photoelectron microscope can be considered to be the electron optics analogue of the fluorescence microscope. UV light from a short arc lamp is focused on the specimen as in fluorescence microscopy but, instead of imaging the emitted fluorescent light with a light optics system, emitted electrons are accelerated and imaged with an electron lens system. Photoelectron microscopy has several advantages, including high sensitivity to topographic detail (3, 6), a new source of contrast based on the photoelectric effect (7–9), and an unusually short depth of information (10). The increase in image quality during the development of the photoelectron microscope over the past few years has been substantial. Although the basic mechanisms by which the photoelectron microscopy image arises are understood, the interpretation of photoelectron microscopy images of biological specimens is the focus of current research. Here we report the comparison of photoelectron micrographs with fluorescence micrographs of the same cells that have been labeled by indirect immunofluorescence techniques with antibodies specific for actin, keratin, or vimentin. The fluorescence micrographs were obtained first and the photoelectron micrographs were obtained second so that the cytoskeletal structures observed by immunofluorescence would be directly comparable with those identified previously in Pt K2 and Rat-1 cells or similar epithelial and fibroblastic cells (11–14).

The publication costs of this article were defrayed in part by page charge payment. This article must therefore be hereby marked "*advertisement*" in accordance with 18 U.S.C. §1734 solely to indicate this fact.

MATERIALS AND METHODS

Antibodies and Cell Lines. Mouse monoclonal antiactin (15) and rabbit antiactin (16) antibodies were provided by J. Lin (Cold Spring Harbor Laboratory, Cold Spring Harbor, NY) and by K. Burridge (University of North Carolina), respectively. I. C. Summerhayes prepared and characterized the rabbit antikeratin antiserum by the method of Sun and Green (17). The preparation and characterization of the mouse monoclonal antibody recognizing vimentin filaments will be described elsewhere (unpublished data). The Pt K2 cell line (CCL 56) is from the American Type Culture Collection and has been described (18). Rat-1 is a normal rat fibroblast cell line (19).

Coverslip Treatment. Conductive substrates, required for photoelectron microscopy, were prepared as follows. To 8.3 ml of ice-cold methanol (100%), 1.7 ml of $SnCl_4$ (100%) was added slowly, and then 0.1 ml of NH_4F_2H (1 g/ml in water) was added. This solution was filtered through a Unipore disc prefilter (Bio-Rad). Clean 5-mm glass coverslips (Bellco Glass) were heated to about 400°C on an aluminum slab and then misted for ≈30 sec on each side with the above solution. The tin oxide-coated coverslips were sterilized by exposure to a germicidal lamp and then incubated with undiluted calf serum at 37°C for 10–60 min. The coverslips were then rinsed in sterile distilled water, air dried, and stored under sterile conditions. Cells were grown on the coated coverslips in Dulbecco's modified Eagle's medium (GIBCO)/10% fetal calf serum (GIBCO) in a 10% CO_2/90% air incubator at 37°C.

Immunofluorescent Labeling. Localization of cytoskeletal elements was carried out by indirect immunofluorescence. For actin-containing stress fibers, cells were fixed in 3.7% formaldehyde in phosphate buffered-saline (P_i/NaCl) for 30 min, washed in P_i/NaCl, and permeabilized with either acetone at −20°C for 2 min or 0.1% Triton X-100 in P_i/NaCl at room temperature for 3 min (for Pt K2 cells, the latter appeared to be preferable and was used in this work). Cells were then stained with rabbit antiactin antibody (for Pt K2) or mouse monoclonal antiactin (for Rat-1) and then with rhodamine-conjugated goat anti-rabbit IgG (Meloy, Springfield, VA) or rhodamine-conjugated goat anti-mouse mixed Igs (Cappel Laboratories, West Chester, PA). For keratin filaments in Pt K2 and vimentin fil-

Abbreviation: P_i/NaCl, phosphate-buffered saline.

aments in Rat-1, cells were fixed and permeabilized in methanol at −20°C for 5 min. After distilled water and P_i/NaCl washes, the cells were stained with rabbit antikeratin (for Pt K2) or mouse monoclonal anti-vimentin (for Rat-1) and then with rhodamine-conjugated goat anti-rabbit IgG (Meloy) or rhodamine-conjugated goat anti-mouse mixed Igs (Cappel). The labeled samples were washed in P_i/NaCl and mounted cell side down on a drop of glutaraldehyde fixative (2.5% glutaraldehyde/0.1 M Na cacodylate/0.1 M sucrose, pH 7.4) in an observation chamber [a silicon rubber sheet punched with 3-mm holes and pressed onto a standard glass microscope slide (20)].

Fluorescence Microscopy. Fluorescence microscopy of the labeled cell samples was carried out with epifluorescence illumination at 546 nm on a Zeiss Photomicroscope III equipped with a Zeiss Planapo 63× objective lens. Exposures were made on Kodak Tri-X film.

Photoelectron Microscopy. After the fluorescence microscopy, the lens immersion oil was carefully cleaned from the back of the coverslip, and the coverslip was transferred to a vial containing the glutaraldehyde fixative described above and stored at 4°C. The fixed samples were dehydrated through a graded series of aqueous ethanol mixtures to 100% ethanol, followed by ethanol/amyl acetate (1:1) and 100% amyl acetate, and then dried under a stream of warm air, as in previous photoelectron microscopy studies on intact cells (1, 2, 5).

The photoelectron microscope used in this study was built at the University of Oregon. It is an ultra-high-vacuum instrument designed to eliminate sample contamination and has been described elsewhere (21). The acceleration voltage was 30 kV; the illumination was provided by two OSRAM HBO 100 W/2 Hg short arc lamps; the objective aperture was 50 μm; the emulsion was Kodak electron image film 4489; and the exposure times varied from 1 to 30 sec.

RESULTS

Fig. 1*a* is a fluorescence micrograph of a small area of a nearly confluent monolayer of rat kangaroo epithelial (Pt K2) cells visualized by immunofluorescence with actin antibody. This micrograph shows the long bundles of actin-containing stress fibers, many of which span the cells and terminate at the cell periphery. The dark area in the upper part of the micrograph is the exposed substrate. Fig. 1*b* is a photoelectron micrograph of the same area. Large numbers of the stress fibers can be traced in both the fluorescence and the photoelectron micrographs and three of these are marked by arrows. Fig. 2*a* is a fluorescence micrograph of a rat fibroblast that has also been visualized by actin antibody. Numerous stress fibers are evident and again most of these can be traced in the photoelectron micrograph (Fig. 2*b*) and its enlargement (Fig. 2*c*). A few are indicated by arrows.

We also investigated two intermediate (10-nm) filament systems, keratin filaments in Pt K2 epithelial cells and vimentin filaments in Rat-1 fibroblasts. The distribution of keratin filaments in a Pt K2 cell is shown in Fig. 3*a*. The long wavy intermingled fibers are known to consist primarily of bundles of individual 10-nm keratin filaments (14). A large number of these fibers can be traced in the corresponding photoelectron micrographs of Fig. 3 *b* and *c* and a few are indicated by arrows in all three micrographs. The arrowhead in Fig. 3*c* points to some internal structure of filaments within a fiber bundle. The apparent diameters of the fibers are less in Fig. 3 *b* and *c* than in Fig. 3*a*, consistent with the much higher resolution of the photoelectron microscope. Vimentin filaments have been reported to occur individually or as loose bundles of fibers (14, 22). The fluorescence micrograph of Fig. 4*a* shows the characteristic network of vimentin filaments in a Rat-1 fibroblast. Many fibers are easily traced in both the fluorescence and higher resolution photoelectron micrographs (Fig. 4 *b* and *c*).

DISCUSSION

The fluorescence and photoelectron micrographs are remarkably similar in appearance considering that the origins of the images are so different and that the specimens have been dehydrated in proceeding from *A* to *B* in Figs. 1–4. The fluo-

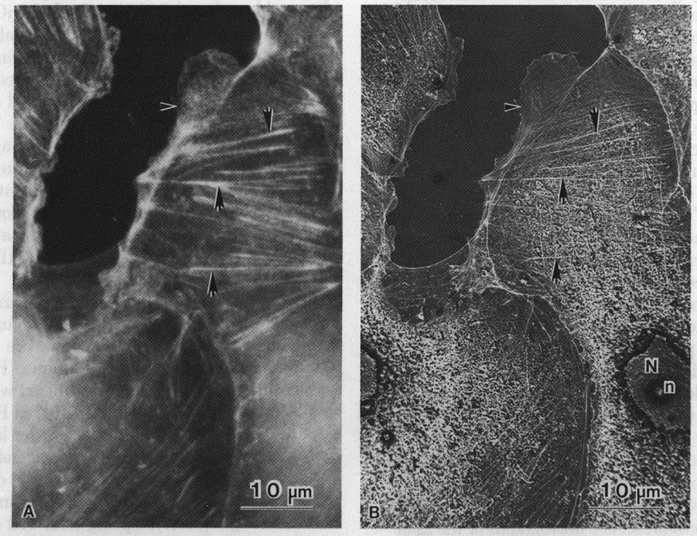

FIG. 1. Fluorescence micrograph (*A*) and photoelectron micrograph (*B*) of the same Pt K2 epithelial cells at comparable magnifications. The cells were prepared for immunofluorescence visualization of actin, photographed in the fluorescence microscope, and then fixed in glutaraldehyde, dehydrated, and photographed in the photoelectron microscope. The arrows point to a few of the actin-containing stress fibers that can be identified in both the fluorescence and the photoelectron micrographs. N and n, nucleus and nucleolus, respectively.

rescence image primarily relies on the contrast between labeled and unlabeled structures whereas the contrast in the photoelectron images here is primarily due to the topography of the sample. Two sources of contrast, material and topographical, can contribute to the imaging of cytoskeletal structures in photoelectron micrographs. Material contrast is provided by differences in photoelectron quantum yield (electrons produced per incident photon) just as contrast in fluorescence microscopy is due to differences in fluorescent quantum yields (7–9). It has been suggested that the photoelectron quantum yields of some dyes might be sufficiently larger than that of the background to permit these dyes to act as photoelectron labels (23–25). However, this type of material contrast was not observed under the experimental conditions used in this study. For example, Fig. 4*b* shows the characteristic pattern of the stress fibers (see the region below the white arrowhead) in addition to the labeled vimentin-containing intermediate filaments (arrows) seen in the fluorescence micrograph. Although the vimentin-containing fibers are decorated with antibodies having one to three rhodamine molecules attached per antibody molecule, they do not appear significantly brighter in the photoelectron micrographs than do the unlabeled stress fibers. The major source of contrast seen in these and previously published photoelectron micrographs of cells is topographical contrast. Photoelectron microscopy is one of the most sensitive surface techniques for imaging fine topographical detail. For example, steps as small as 3 nm have been detected (26). This sensitivity occurs because the electrons emerging from the specimen have very low kinetic energies before acceleration and are easily deflected by small variations in the electric field, such as those produced by sample topography (3, 6). It also places a limitation on the technique. Specimens that have large variations in topography can exceed the useful range and induce obvious distortions in the photoelectron microscopy images. This might occur with some cell preparations, but the cytoskeletal elements and other structural features observed on these specimens and in previous photoelectron microscopy studies (1, 2, 5) are well within the range of this technique.

Photoelectron microscopy and fluorescence microscopy also differ in the depth of information. Photoelectron microscopy is a surface technique with very high depth resolution (short depth of information) because only those electrons that are photoionized at or very near the surface can escape from the specimen to form the image (10). In the cells used here, the majority of stress fibers occur on the cytoplasmic face of the lower cell surface, although they also occur throughout the cell. The fluorescence micrographs of Figs. 1 and 2 were taken in the substrate plane of focus. Therefore, of the stress fibers shown in the fluorescence micrographs, only those that are either exposed in the preparative procedures (for instance, the process of rendering the cells permeable to the antibodies) or lie directly under the cell surface and cause ridges are visualized in the photoelectron micrographs. In this aspect, the techniques are complementary. For the same reasons, differences between the fluorescence and photoelectron micrographs can also be seen in and around the nuclear regions. The photoelectron micrographs show a jumbled surface (presumably caused by partially collapsed and aggregated cellular components) surrounding sharply defined nuclei whereas, in the corresponding fluorescence micrographs, the nuclei are unlabeled and consequently appear diffuse.

Another difference between fluorescence and photoelectron microscopy is the resolution in the image. The resolution of the optical microscope is limited to about 200 nm by the wavelength of the emitted light whereas the resolution of the photoelectron microscope is determined by the wavelength of the *emitted electrons* plus aberrations in the electron optics system. The resolution of this photoelectron microscope in its present configuration is on the order of 10–20 nm and may reach the design goal of 5 nm when completed (13). The higher resolving power of photoelectron microscopy is evident in all four figures. Fluorescence micrographs give the overall impression that the cytoskeletal structures occupy a much larger fraction of the cytoplasmic space whereas photoelectron micrographs show these

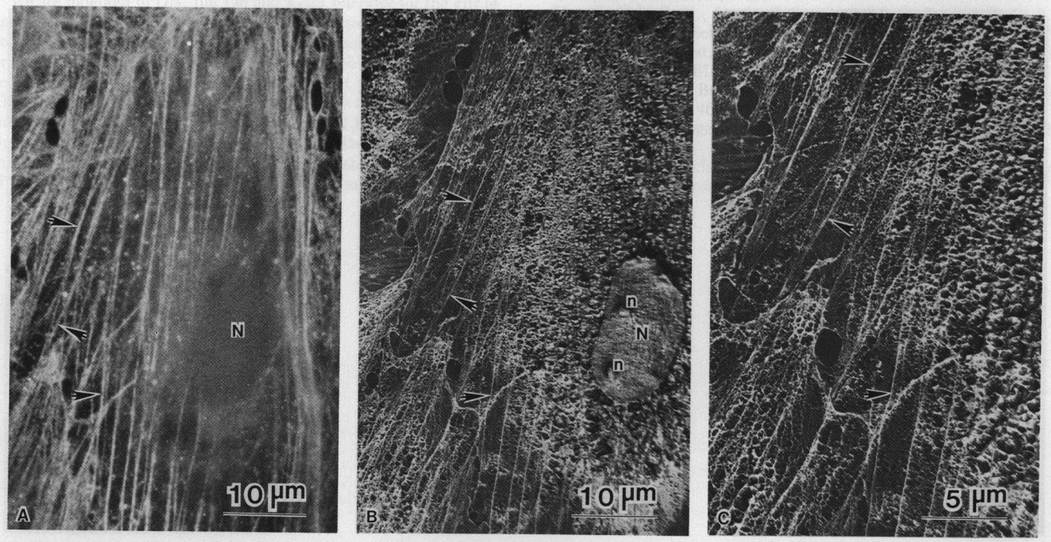

FIG. 2. Fluorescence micrograph (*A*) and photoelectron micrographs (*B* and *C*) of the same Rat-1 fibroblasts. As in Fig. 1, the cells were prepared for immunofluorescence visualization of actin. The arrows identify a few of the same stress fibers clearly seen by both fluorescence and photoelectron microscopy. *C* is an enlargement of a portion of *B*. The nucleus (N) contains several nucleoli (n).

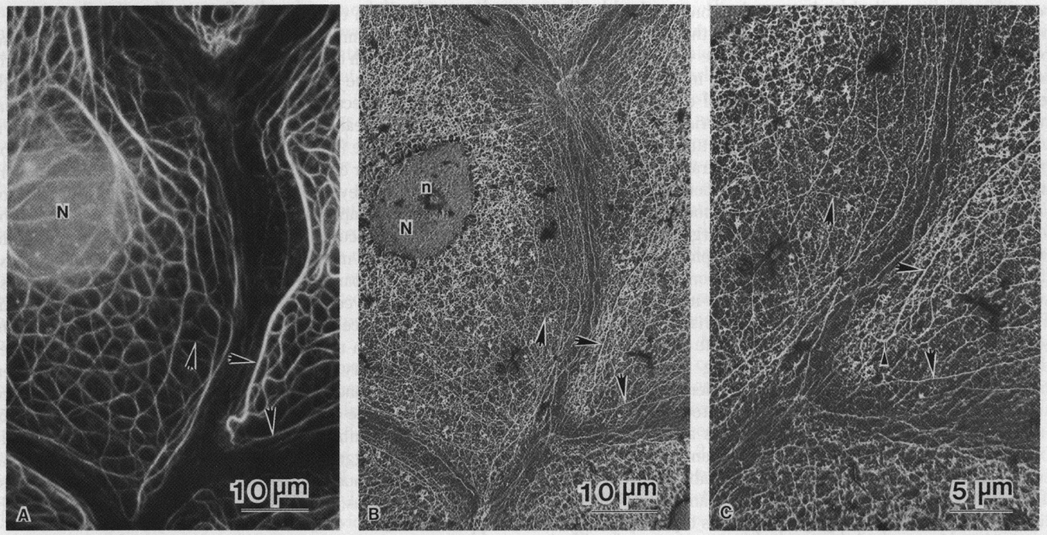

FIG. 3. Pt K2 epithelial cells prepared for immunofluorescent visualization of keratin. (*A*) Fluorescence micrograph. (*B*) Photoelectron micrograph. (*C*) An enlargement of a portion of *B*. The arrows mark some of the bundles of keratin filaments identifiable by both techniques.

structures at more nearly their true dimensions. For example, in Fig. 3 the smallest keratin fibers that can be traced in both types of micrographs have diameters of ≈30 nm in the photoelectron micrographs. For comparison, a single keratin filament fully decorated with two layers of antibodies would be ≈46 nm in diameter (i.e., a 10-nm filament plus four 9-nm antibodies), assuming the long axes of the antibodies are perpendicular to the filament. This difference is not large and can be accounted for by several factors, including incomplete decoration, tilting of the antibodies, or dehydration effects occurring during specimen preparation for photoelectron microscopy. These same fibers are visible in the fluorescence micrograph because of the high contrast provided by the fluorescent markers, but they are imaged at a minimum diameter of roughly 200 nm, the resolution limit of the optical microscope. Similarly, the smallest vimentin fibers measured in the photoelectron micrographs that can also be located in the fluorescence micrographs are ≈30 nm, again consistent with single fibers deco-

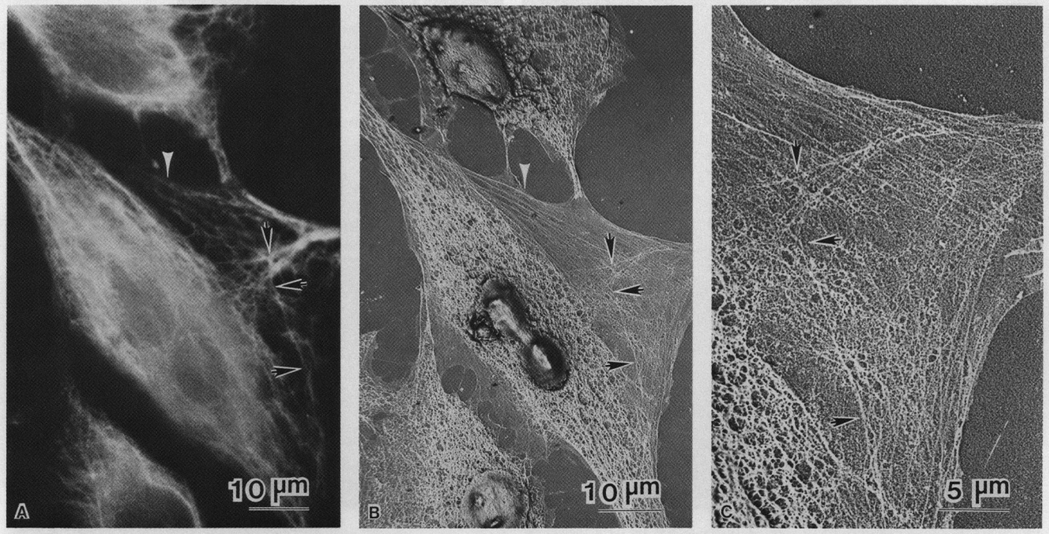

FIG. 4. Rat-1 fibroblast prepared for immunofluorescent visualization of vimentin. Vimentin filaments (arrows) are seen in both the fluorescence (*A*) and photoelectron (*B* and *C*) micrographs whereas stress fibers (e.g., region near the arrowheads in *A* and *B*) are visible only in the photoelectron micrographs.

rated with antibodies. Thus, it may be possible to detect a single intermediate filament in a whole-mount specimen by photoelectron microscopy. Observations of single filaments with dimensions much smaller than the resolution of the fluorescence microscope have been well documented in comparisons of immunofluorescence and transmission electron microscopy of the same Pt K2 cells (13, 18).

In conclusion, we have shown here that it is feasible and instructive to carry out fluorescence and photoelectron microscope studies on the same cells. Many cytoskeletal elements that were labeled and visualized by fluorescence microscopy in these preparations were also detected by photoelectron microscopy by virtue of the mechanism of topographical contrast. The high depth resolution (short depth of information) that makes photoelectron microscopy a uniquely surface-sensitive technique means that the cytoskeleton will only be detected in areas where the cell surface has either been disrupted or the underlying structures are so closely apposed to it that the topography of the cells surface reflects their presence. Relating the comparisons of Figs. 1–4 to previous photoelectron microscopy studies suggests that the cytoskeletal structures most often seen in photoelectron microscopy of whole cells are stress fibers (5). Besides placing the interpretation of photoelectron micrographs on a firmer basis, these results provide some insight into how photoelectron microscopy will be useful in future experiments in cell biology. The very high sensitivity to fine topographical detail makes exposed surface structures clearly visible in the photoelectron images without the need for staining the preparation. No metal or other conductive coating is required, eliminating one possible source of loss of resolution and contrast. Furthermore, as photoemission labels for photoelectron microscopy are developed and come into use (5), it should be possible to enhance contrast of specific cytoskeletal elements or cell surface components while still observing the remaining structures. For these reasons, photoelectron microscopy promises to provide useful and unique complementary information to that attainable by more established microscope techniques.

We are indebted to Drs. Jim Lin and Keith Burridge for the gift of antibodies and to George H. Lesch and Dr. Gertrude F. Rempfer for continued improvement of the University of Oregon photoelectron microscope. We acknowledge useful discussions with Drs. G. Bruce Birrell, Patricia C. Jost, Klaus Weber, Mary Osborn, and Suh Der Tsen. This work was supported by Grants CA-11695 (to O.H.G.) and CA-22659 (to L.B.C.) from the National Cancer Institute. K.K.N. was supported by a National Cancer Institute Training Grant to Dr. A. B. Pardee during 1981 and by an American Cancer Society Postdoctoral Fellowship (PF-2105) during 1982 and is currently the recipient of a National Cancer Institute Postdoctoral Fellowship (CA-070407-01). L.B.C. is supported by an American Cancer Society Faculty Research Award.

1. Dam, R. J., Nadakavukaren, K. K. & Griffith, O. H. (1977) *J. Microsc. (Oxford)* **111,** 211–217.
2. Nadakavukaren, K. K., Rempfer, G. F. & Griffith, O. H. (1981) *J. Microsc. (Oxford)* **122,** 301–308.
3. Schwarzer, R. A. (1981) *Microsc. Acta* **84,** 51–86.
4. Griffith, O. H., Brown, H. M. & Lesch, G. H. (1978) in *Light Transducing Membranes: Structure, Function and Evolution*, ed. Deamer, D. (Academic, New York), pp. 313–334.
5. Griffith, O. H., Rempfer, G. F. & Nadakavukaren, K. K. (1982) in *Electron Microscopy*, Proceedings of the Tenth International Congress on Electron Microscopy, ed. Le Poole, J. B. (Deutsche Gesellschaft f. Elektronenmikroskopie, e.V., Frankfurt), Vol. 1, pp. 59–68.
6. Rempfer, G. F., Nadakavukaren, K. K. & Griffith, O. H. (1980) *Ultramicroscopy* **5,** 437–448.
7. Dam, R. J., Kongslie, K. F. & Griffith, O. H. (1974) *Biophys. J.* **14,** 933–939.
8. Barnes, R. B., Amend, J., Sistrom, W. R. & Griffith, O. H. (1978) *Biophys. J.* **21,** 195–202.
9. Houle, W. A., Brown, H. M. & Griffith, O. H. (1979) *Proc. Natl. Acad. Sci. USA* **76,** 4180–4184.
10. Houle, W. A., Engel, W., Willig, F., Rempfer, G. F. & Griffith, O. H. (1982) *Ultramicroscopy* **7,** 371–380.
11. Lazarides, E. (1980) *Nature (London)* **283,** 249–256.
12. Lazarides, E. & Weber, K. (1974) *Proc. Natl. Acad. Sci. USA* **71,** 2268–2272.
13. Webster, R. E., Osborn, M. & Weber, K. (1978) *Exp. Cell Res.* **117,** 47–61.
14. Henderson, D. & Weber, K. (1981) *Exp. Cell Res.* **132,** 297–311.
15. Lin, J.-C. (1981) *Proc. Natl. Acad. Sci. USA* **78,** 2335–2339.
16. Burridge, K. (1976) *Proc. Natl. Acad. Sci. USA* **73,** 4457–4461.
17. Sun, T.-T. & Green, H. (1978) *Cell* **14,** 469–476.
18. Osborn, M., Webster, R. E. & Weber, K. (1978) *J. Cell Biol.* **77,** R27–R34.
19. Cheng, Y.-S. E. & Chen, L. B. (1981) *Proc. Natl. Acad. Sci. USA* **78,** 2388–2392.
20. Johnson, L. V., Walsh, M. L. & Chen, L. B. (1980) *Proc. Natl. Acad. Sci. USA* **77,** 990–994.
21. Griffith, O. H., Rempfer, G. F., Lesch, G. H. (1981) *Scanning Electron Microscopy* **2,** 123–130.
22. Goldman, R. D. & Knipe, D. M. (1972) *Cold Spring Harbor Symp. Quant. Biol.* **27,** 523–534.
23. Griffith, O. H., Lesch, G. H., Rempfer, G. F., Birrell, G. B., Burke, C. A., Schlosser, D. W., Mallon, M. H., Lee, G. B., Stafford, R. G., Jost, P. C. & Marriott, T. B. (1972) *Proc. Natl. Acad. Sci. USA* **69,** 561–565.
24. Birrell, G. B., Burke, C., Dehlinger, P. & Griffith, O. H. (1973) *Biophys. J.* **13,** 462–469.
25. Grund, S., Engel, W. & Teufel, P. (1975) *J. Ultrastruct. Res.* **50,** 284–288.
26. Reimer, L., Schulte, E., Schulte, C. & Schur, K. (1972) *Beitr. elektronenmikroskop. Direktabb. Oberfl.* **5,** 987–1006.